

Syringolin A Selectively Labels the 20S Proteasome in Murine EL4 and Wild-Type and Bortezomib-Adapted Leukaemic Cell Lines

Jérôme Clerc,^[a] Bogdan I. Florea,^[b] Marianne Kraus,^[c] Michael Groll,^[d] Robert Huber,^[e, f, g] André S. Bachmann,^[h] Robert Dudler,^[i] Christoph Driessen,^[c] Herman S. Overkleeft,^[b] and Markus Kaiser^{*[a]}

The natural product syringolin A (SylA) is a potent proteasome inhibitor with promising anticancer activities. To further investigate its potential as a lead structure, selectivity profiling with cell lysates was performed. At therapeutic concentrations, a rhodamine-tagged SylA derivative selectively bound to the 20S proteasome active sites without detectable off-target labelling. Additional profiling with lysates of wild-type and bor-

tezomib-adapted leukaemic cell lines demonstrated the retention of this proteasome target and subsite selectivity as well as potency even in clinically relevant cell lines. Our studies, therefore, propose that further development of SylA might indeed result in an improved small molecule for the treatment of leukaemia.

Introduction

The ubiquitin–proteasome pathway regulates numerous cellular processes, such as cell growth, apoptosis or differentiation.^[1] The 20S proteasome represents the proteolytic core system of this pathway. It is a multiprotein complex consisting of 28 subunits arranged in a $\alpha_7\beta_7\beta_7\alpha_7$ manner and harbours three distinct proteolytic sites: a chymotryptic-like activity in the $\beta 5$ subunit, a tryptic-like activity in $\beta 2$, and a caspase-like activity located at the $\beta 1$ subunit.^[2] In immune-competent cells, an alternative proteasome species known as the immunoproteasome is expressed in addition to the constitutive proteasome upon γ -interferon stimulation. In the immunoproteasome, the $\beta 1$, $\beta 2$ and $\beta 5$ subunits are replaced by $\beta 1i$, $\beta 2i$, and $\beta 5i$, respectively.^[3]

Proteasome inhibitors have proven to be valuable anticancer agents as exemplified by bortezomib (Velcade®), the first proteasome inhibitor approved by the FDA for the treatment of refractory and/or relapsed multiple myeloma and mantle cell lymphoma.^[4] In addition, clinical trials with three more chemical entities, that is, NPI-0052, CEP-18770 and carfilzomib, are currently underway.^[5] However, bortezomib treatment is hampered by the occurrence of side effects and tumour resistance arising from mutations in the inhibitor binding pockets or by over-expression of “rescue” proteases, such as TPPII, during therapy.^[6] Consequently, a medical need for structurally diverse proteasome inhibitors still exists.

The screening of natural products followed by their organic synthesis has resulted in the identification of several potent proteasome inhibitors.^[7] Recently, we reported the elucidation of a new class of proteasome inhibitors, the syrbactins.^[8] The syrbactins unify two structurally related natural product families: the syringolins, which are produced by strains of the plant pathogen *Pseudomonas syringae* pv. *syringae*, and the glidobac-

tins, which are produced by an unknown species of the order *Burkholderiales* (Scheme 1 A). Both natural product families contain an α,β -unsaturated amide functionality that is irreversibly

[a] J. Clerc, Dr. M. Kaiser

Chemical Genomics Centre der Max-Planck-Gesellschaft
Otto-Hahn-Strasse 15, 44227 Dortmund (Germany)
Fax: (+49) 231-9742-6479
E-mail: markus.kaiser@cgc.mpg.de

[b] B. I. Florea, Prof. Dr. H. S. Overkleeft

Leiden Institute of Chemistry and Netherlands Proteomics Centre
Gorlaeus Laboratories, Einsteinweg 55
2333 CC Leiden (The Netherlands)

[c] M. Kraus, Prof. Dr. C. Driessen

Cantonal Hospital St. Gallen, Laboratory for Experimental Oncology
Rorschacherstrasse 95, 9007 St. Gallen (Switzerland)

[d] Prof. Dr. M. Groll

Centre for Integrated Protein Science at the Department of Chemistry
Technische Universität München
Lichtenbergstrasse 4, 85747 Garching (Germany)

[e] Prof. Dr. R. Huber

Max-Planck-Institut für Biochemie
Am Klopferspitz 18 a, 82152 Martinsried (Germany)

[f] Prof. Dr. R. Huber

Zentrum für Medizinische Biotechnologie, Universität Duisburg–Essen
45117 Essen (Germany)

[g] Prof. Dr. R. Huber

School of Biosciences, Cardiff University
Cardiff CF10 3US (UK)

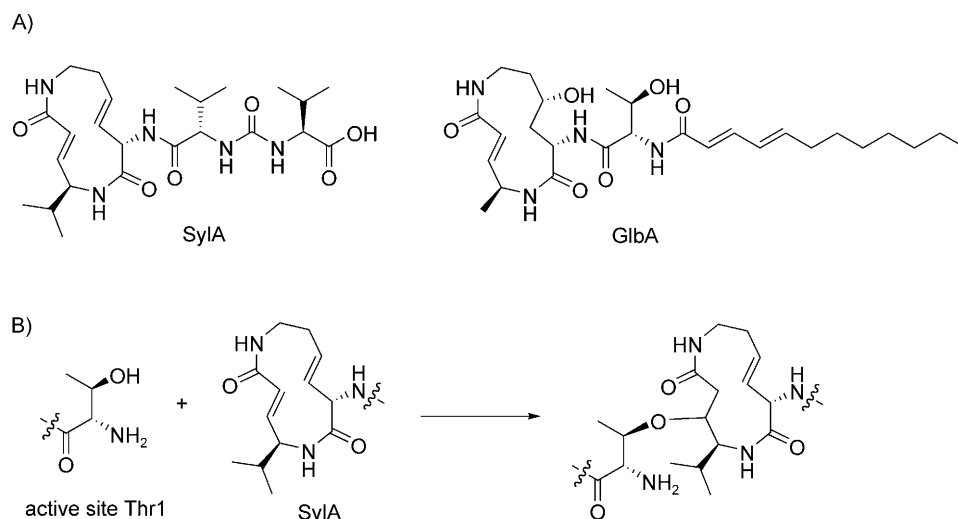
[h] Prof. Dr. A. S. Bachmann

Cancer Research Center of Hawaii, University of Hawaii at Manoa
1236 Lauhala Street, 96813 Honolulu, Hawaii (USA)

[i] Prof. Dr. R. Dudler

Zürich–Basel Plant Science Centre, Institute of Plant Biology
Universität Zürich, Zollikerstrasse 107, 8008 Zürich (Switzerland)

Supporting information for this article is available on the WWW under <http://dx.doi.org/10.1002/cbic.200900411>.



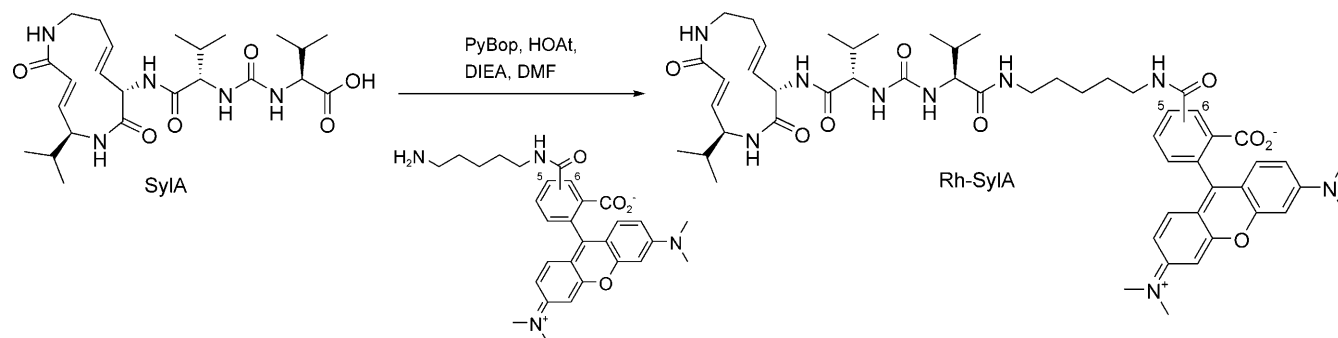
Scheme 1. A) Chemical structures of syrbactins syringolin A (SylA) and glidobactin A (GlbA). B) The threonine active site of the 20S proteasome reacts with SylA in a Michael-type addition; this leads to irreversible inhibition.

attacked in a Michael-type addition by the O^γ of the 20S proteasome active site residue threonine; thereby a covalent ether bond is formed (Scheme 1B). A first analysis of the structure–activity relationships (SAR) of the syrbactins revealed that proteasome inhibitors based on the syringolin A (SylA) scaffold can bind to all three proteolytic activities of the proteasome while glidobactin targets only the tryptic- (β 2) and chymotryptic-like (β 5) activities.^[9] To date, it is not known whether this also applies to the immunoproteasome as no biochemical assays of a syrbactin with the immunoproteasome have been performed.

The parent natural product SylA is a promising anticancer agent that both inhibits growth and induces apoptosis of neuroblastoma and ovarian cancer cells.^[10] However, further development of syringolin-based compounds into anticancer agents might be hampered by two unwanted side effects: 1) SylA's reactive Michael acceptor system could cross-react with other nucleophilic enzymes, such as cysteine proteases, and thereby cause unwanted side effects, and 2) SylA might display only a low reactivity and thereby have limited efficiency in bortezomib-resistant cells due to mutations of the 20S proteasome active site. In order to gain an answer to these two critical questions, we initiated a chemical biology study that capital-

this end, peptide coupling of an amino pentane rhodamine precursor with the free carboxylic acid moiety of either isolated or synthetic syringolin A was performed; this yielded the desired probe Rh-SylA in good overall yield (Scheme 2). The carboxyl group was chosen as previous SAR indicated that this functional group is amenable to modification without significant loss of inhibitory potency.^[9]

With the Rh-SylA probe in hand we set out to establish its labelling behaviour in a biological sample. For this purpose, we prepared Rh-SylA dilutions in the concentration range 10 nM to 10 μ M and incubated these for 1 h at 37 °C with protein (20 μ g) from EL4 cell lysates before addition of MS076 (1 μ M) and incubation for 1 h at 37 °C. MS076 (Figure 1C) is a characterised green fluorescent BODIPY-tagged epoxomicin proteasome probe and can be visualised selectively at distinct wavelengths that do not interfere with the rhodamine-derived red fluorescence of Rh-SylA.^[12e] EL4 is a murine cell line that expresses both the constitutive and the immunoproteasome β subunits. The left panel of Figure 1A shows the fluorescent signals for rhodamine detection resulting from Rh-SylA binding. Labelling was detectable at a concentration of 50 nM Rh-SylA and increased gradually in a concentration-dependent manner until saturation was reached at around 5 μ M. Above



Scheme 2. Synthesis of the fluorescent Rh-SylA probe.

ised on SylA's irreversible, covalent binding mode, and used a SylA-derived probe for activity-based protein profiling (ABPP).^[11]

Results

To date, ABPP has been widely used to determine enzyme activity states of complex proteomes in vitro and in vivo, and several proteasome-specific probes with different tag systems have already been reported.^[12] To facilitate our later profiling experiments, we chose to develop a SylA-based probe with a fluorescent rhodamine tag that allows straightforward in-gel fluorescence detection. To

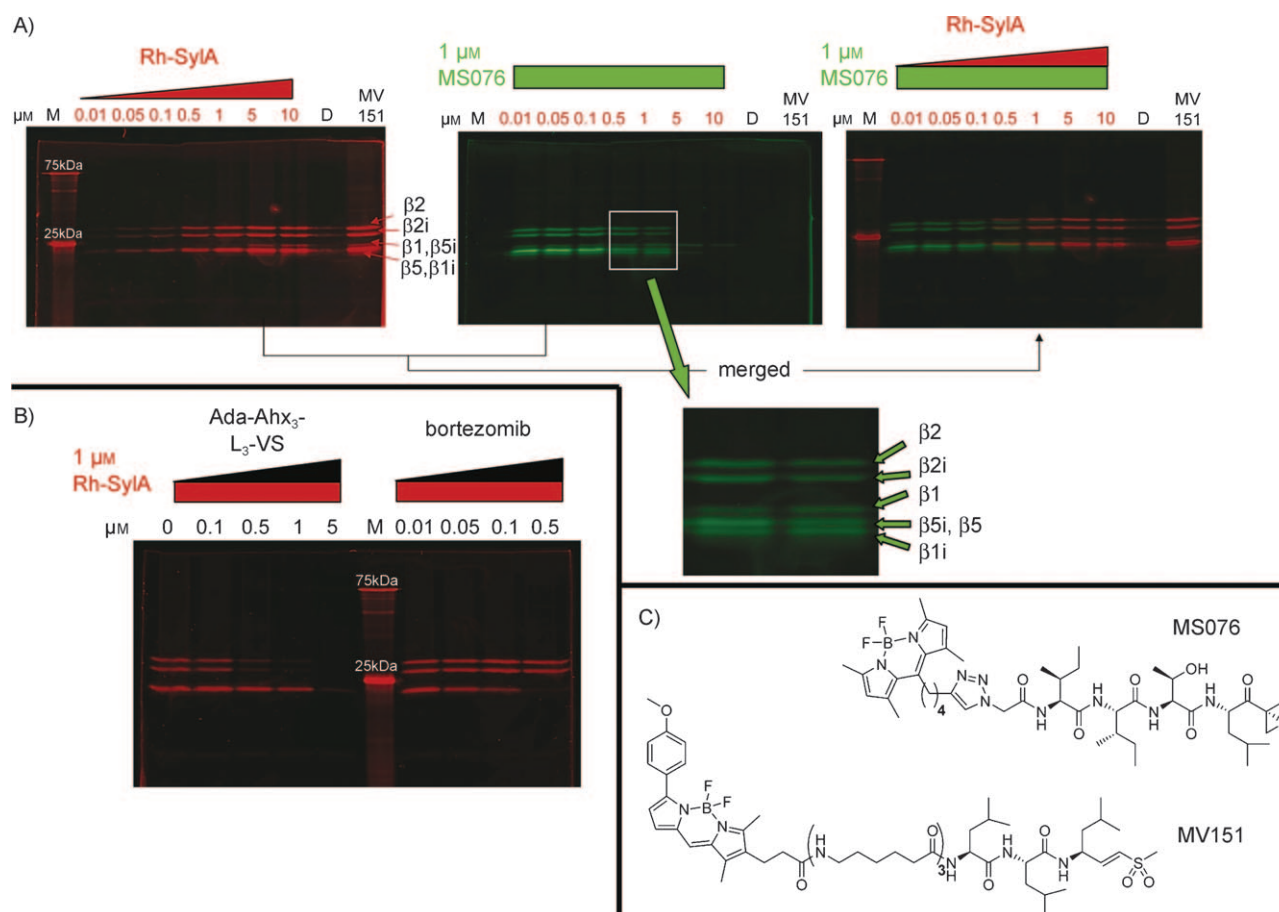


Figure 1. In-gel fluorescence analysis of Rh-SylA-labelled murine EL4 cell lysates (20 μg protein per lane) in the presence and absence of known proteasome inhibitors or ABP. A) Concentration-dependent labelling of the proteasome by Rh-SylA. EL4 lysate was incubated with increasing concentrations of Rh-SylA for 1 h at 37 °C, followed by 1 h incubation with MS076 (1 μM) to reveal residual proteasome activity. The left panel shows the red rhodamine channel, corresponding to Rh-SylA (λ_{ex} = 523 nm, λ_{em} = 580 nm), the central panel corresponds to MS076 and the green BODIPY-FL channel (λ_{ex} = 488 nm, λ_{em} = 520 nm), and the right panel is the merged image. The magnification shows the identity of the MS076-labelled proteasome β subunits. Denatured (D) lysate and proteasome labelling with MV151 were used as negative and positive controls, respectively. B) Competition assay with Rh-SylA (1 μM) in the presence of varying concentrations of the known proteasome inhibitors Ada-Ahx₃-L₃-VS and bortezomib. C) Chemical structures of MV151 and MS076; M: protein molecular weight marker.

1 μM of Rh-SylA, four distinct bands were visible that resembled the profiling pattern obtained with the archetypical MV151 proteasome activity probe (Figure 1A, left panel and Figure 1C; for gel loading controls see the Supporting Information).^[12d] It is worth noting that Rh-SylA interfered with both the constitutive proteasome and the immunoproteasome catalytic β subunits. Also, the excellent signal-to-noise ratio of Rh-SylA labelling is striking. Importantly, the denatured control sample for activity and specificity (lane 9: SDS treated and heat denatured EL4 lysate incubated with 10 μM Rh-SylA) resulted in no significant bands. Altogether, our findings demonstrate that the SylA-derived probe is indeed very specific for the proteasome.

To further characterise the potency and specificity of Rh-SylA, we also analysed the resulting green BODIPY-derived fluorescence of MS076 from the same experiment (Figure 1A, central panel). As expected, the MS076 fluorescence decreased with increasing Rh-SylA concentration; this indicates competition between the two compounds for the same protein target—the proteasome β subunits. Fluorescence detection of

MS076 allowed a better resolution of the β 1, β 1i, β 5 and β 5i subunits (Figure 1A, magnification of central panel); this reveals that Rh-SylA completely blocked the β 2 and β 2i subunits at 5 μM while a SylA concentration of 10 μM was necessary to fully inhibit the β 1i subunit. From the merged picture of the green and red signal (Figure 1A, right panel) the identity of Rh-SylA and MS076-labelled bands becomes apparent, although the Rh-SylA-labelled bands resolve at a slightly higher molecular weight than the MS076-labelled bands due to the higher molecular weight of Rh-SylA. This experiment clearly demonstrates that Rh-SylA is a potent and specific proteasome activity-based probe (ABP).

We next set out to elucidate if Rh-SylA is a suitable ABP for the assessment of the efficacy in proteasome inhibition of other untagged inhibitors. For this purpose we chose the proteasome inhibitors Ada-Ahx₃-L₃-VS and bortezomib. Protein (20 μg) from EL4 lysates were first incubated with increasing concentrations of competitors for 1 h at 37 °C and the residual proteasome activity was visualised by Rh-SylA. Figure 1B shows that Ada-Ahx₃-L₃-VS first bound to the β 2 and β 2i

subunits and finally at a concentration of 5 μM all proteasome activity was silenced. In contrast, bortezomib efficiently blocked the constitutive and $\beta 1$ and $\beta 5$ immunosubunits without inhibiting the $\beta 2$ or $\beta 2i$ subunits. Importantly, the observed difference in competition efficiency of Ada-Ahx₃-L₃-VS and bortezomib is in agreement with their known different inhibitory potency. For example, Ada-Ahx₃-L₃-VS binds more efficiently to $\beta 2$ and $\beta 2i$ proteasome subunits than bortezomib, while bortezomib efficiently targets the $\beta 1$, $\beta 1i$, $\beta 5$ and $\beta 5i$ subunits.^[13]

We next investigated if Rh-SyIA also selectively labels the proteasome in human leukaemia cell lines. Towards this purpose, protein (40 μg) from total cell lysates of parental and bortezomib-adapted HL60 (myeloid leukemia), ARH77 (plasmacytoid lymphoma) and AMO-1 (myeloma) cell lines were incubated with Rh-SyIA and profiled for active proteasome subunits (Figure 2, for loading control see the Supporting Informa-

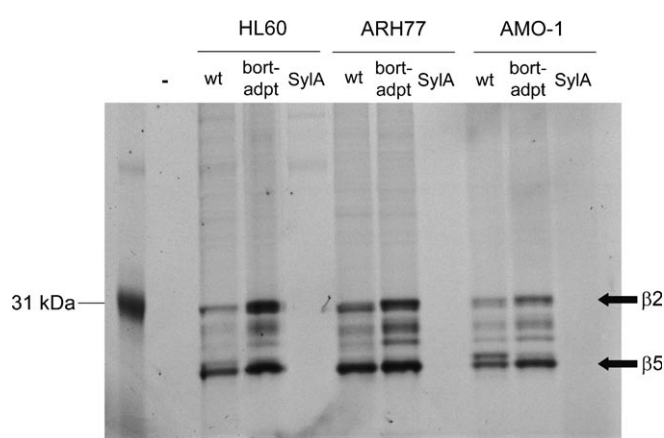


Figure 2. Profiling with Rh-SyIA in wild-type (wt) and bortezomib-adapted (bort-adpt) HL60, ARH77 and AMO-1 leukaemia cell lines. Unlabelled SyIA (SyIA) was used as negative control in all three wild-type cell lines.

tion).^[14] In contrast to wild-type cells, bortezomib-adapted cell lines incubated continuously with increasing bortezomib concentrations have been shown: 1) to retain detectable activity of the $\beta 1$ and $\beta 5$ subunits in the presence of therapeutic concentrations of the drug, and 2) to increase $\beta 2$ activity by ten-fold; this renders bortezomib ineffective in anticancer therapy.^[14] Maintenance of the proteolytic activity of $\beta 5$ in the presence of bortezomib has been attributed to a $\beta 5$ resistance mutation that prevents effective bortezomib binding to the active site.^[15] Rh-SyIA profiling of these cell lines revealed an efficient and selective proteasome labelling, similar to the pattern derived from profiling with MV151 (see the Supporting Information). As expected from the previous EL4 profiling experiments and biochemical inhibition data, binding was most efficient at $\beta 5$ and $\beta 2$. Besides the proteasome-derived bands, no further protein bands appeared; this again indicates selective labelling of the proteasome even in bortezomib-adapted cells. Moreover, a visual comparison of the labelling efficiency of the parental and the bortezomib-adapted cell lines revealed an effective labelling of the critical $\beta 5$ subunit in bortezomib-adapted cell lines.

Discussion

Proteasome inhibitors have demonstrated clinical potential as potent anticancer agents. Although a first proteasome inhibitor (bortezomib) has already been introduced to the clinic, resistance to bortezomib therapy still represents a major challenge for effective chemotherapy; this calls for alternative proteasome inhibitors.

Here, we demonstrated that Rh-SyIA, which is a structurally close analogue of SyIA, selectively labels the proteolytic subunits of the 20S proteasome in a dose-dependent manner. Even at a concentration of 10 μM Rh-SyIA, which is well above typical cellular concentrations of proteasome inhibitors employed during cancer therapy, still no off-target labelling could be detected. As expected from the biochemical inhibition assays of SyIA with human 20S proteasome, Rh-SyIA bound most efficiently to the $\beta 5$ subunit, followed by the $\beta 2$ subunit while binding to $\beta 1$ was much weaker; this is in agreement with previous results. Interestingly, Rh-SyIA labelling of the $\beta 2i$ subunit was almost as strong as $\beta 2$ labelling; this indicates a very high affinity to this subsite as the immunoproteasome usually is expressed at much lower concentrations than the constitutive proteasome. On the contrary, the $\beta 5i$ subunit was much less efficiently labelled than the $\beta 5$ subunit and also $\beta 1i$ was labelled only faintly. To further assure a correct assignment of the visualised active proteasome subunits, the corresponding well-characterised labelling pattern of MS076 was visualised on the same gel (Figure 1A, central panel) by using fluorescence detection at BODIPY-specific wavelengths. The merging of these two analyses unequivocally demonstrated the correct assignment of Rh-SyIA labelling, and pinpoints to a selective targeting of the 20S proteasome in complex proteomes. Importantly, in all performed experiments in the murine EL4 cell line, no other bands resulting from off-target labelling appeared within the used concentration range, and we conclude that Rh-SyIA is both an efficient and highly selective proteasome ABP that might find application in screening assays aimed at the identification of new proteasome inhibitors.

The observed subsite selectivity of Rh-SyIA and thus of SyIA might be of relevance for its anticancer potential. Previous investigations have suggested that efficient inhibition of at least two proteolytic proteasomal subsites is required for an anticancer effect.^[16] While bortezomib preferentially targets the $\beta 5$ and $\beta 1$ subunits, SyIA blocks $\beta 5$ and $\beta 2$ with high potencies, and thus displays a different subsite selectivity pattern, which might be less prone to resistance mutations. In addition, bortezomib resistant cell lines rely heavily on the $\beta 2$ proteolytic activity that can be efficiently targeted with SyIA-derived inhibitors.

As the reactive α, β -unsaturated carbonyl system in principle could also react with the usually more reactive cysteine proteases, the observed selective labelling must be a consequence of its unusual structure. We assume that the macrocyclic ring structure is a major determinant of this selectivity as it exploits a rather unique structural feature of the 20S proteasome. In the 20S proteasome, the S2 as well as S4 pockets of the proteasome are partly solvent exposed.^[2a] This enables the

accommodation of active-site inhibitors that are side-chain cyclised, for example, by the P1 and P2 residue as in the case of SylA or the P2 and P4 residue as for TMC-95A.^[17] In most other proteases, this arrangement, however, causes highly unfavourable steric clashes, which probably explains the observed selectivity.

Importantly, Rh-SylA also showed a promising labelling activity of clinically relevant leukaemia cell lines, including cell lines derived from bortezomib-adapted cells. The labelling efficiency of the different subsites of wild-type and bortezomib-adapted cells was in all three cell lines almost equally efficient. This demonstrates that active-site mutations arising under bortezomib treatment do not seem to affect SylA's preferential binding to the $\beta 5$ and $\beta 2$ subunits of bortezomib-adapted leukaemia cell lines.

Based on these findings and in conjunction with the previous selectivity studies, we propose that syringolin A-based small molecules might indeed represent a suitable structure class for the development of a second generation of proteasome inhibitors for the treatment of leukaemia.

Experimental Section

Synthesis of Rh-SylA: SylA (7.85 mg, 15.9 μmol , 1 equiv) was dissolved in *N,N*-dimethylformamide (2 mL) in a flask (10 mL) and cooled to 0 °C. A solution of a commercially available mixture of 5- and 6-rhodamine amine (30.7 mg, 55.7 μmol , 3.5 equiv), PyBop (24.8 mg, 47.7 μmol , 3 equiv), HOAt (6.5 mg, 47.7 μmol , 3 equiv) and *N,N*-diisopropylethylamine (13.9 μL , 79.5 μmol , 5 equiv) in *N,N*-dimethylformamide (1 mL) were added, and the resulting mixture was stirred for 48 h at room temperature. After evaporation to dryness, the remaining residue was purified by preparative HPLC (solvent A: H_2O with 0.1% TFA, solvent B: acetonitrile with 0.1% TFA; flow: 25 mL min^{-1} ; gradient: from 0 to 10 min: 80% A/20% B; from 10 to 20 min: from 80% A/20% B to 50% A/50% B; from 20 to 50 min: from 50% A/50% B to 35% A/75% B; from 50 to 70 min: from 35% A/75% B to 0% A/100% B; from 70 to 80 min: 0% A/100% B) to yield Rh-SylA (1.42 mg, 1.4 μmol , 9%) as a purple solid.

TLC (25% methanol in chloroform) $R_f = 0.49$; HPLC $t_R = 6.78$ min; $^1\text{H NMR}$ (500 MHz, $[\text{D}_6]\text{DMSO}$) $\delta = 8.71\text{--}8.74$ (m, 1H), 8.17–8.21 (m, 2H), 8.02 (d, $J = 8.7$ Hz, 1H), 7.96 (s, 2H), 7.91 (d, $J = 6.9$ Hz, 1H), 7.84–7.87 (m, 1H), 7.72–7.74 (m, 1H), 7.62 (d, $J = 7.5$ Hz, 1H), 7.41–7.47 (m, 2H), 7.16–7.19 (m, 2H), 7.11–7.13 (m, 1H), 6.95–6.97 (m, 2H), 6.69 (dd, $J = 15.0, 5.7$ Hz, 1H), 6.25–6.31 (m, 2H), 6.10 (d, $J = 15.5$ Hz, 1H), 5.56–5.63 (m, 1H), 5.38–5.44 (m, 1H), 5.32–5.35 (m, 2H), 4.84–4.88 (m, 1H), 4.01–4.10 (m, 2H), 3.91–3.96 (m, 1H), 3.09–3.16 (m, 2H), 3.00–3.06 (m, 4H), 2.90 (s, 6H), 2.74 (s, 6H), 2.24–2.32 (m, 1H), 1.94–2.04 (m, 3H), 1.70–1.78 (m, 1H), 1.44–1.60 (m, 5H), 0.95 (d, $J = 6.8$ Hz, 3H), 0.91 (d, $J = 6.4$ Hz, 3H), 0.77–0.88 (m, 12H); HRMS (ESI) m/z calcd for $\text{C}_{54}\text{H}_{71}\text{O}_9\text{N}_9\text{H}^+$ $[M + \text{H}]^+$ 990.5448, found 990.5457.

Rh-SylA labelling: Rh-SylA labelling with lysates of murine EL4 cell lines was essentially performed as described in ref. [12d] while the Rh-SylA labelling with lysates of wild-type and bortezomib-adapted leukaemia cell lines was carried out according to ref. [14].

In brief, Rh-SylA was employed for labelling experiments by using total cell lysates of the murine cell line EL4 (Figure 1, gel loading controls are shown in the Supporting Information).^[12d] Increasing amounts of Rh-SylA were added to EL4 lysate (10 μL , 20 μg pro-

tein) and incubated for 1 h at 37 °C and boiled with sample buffer (4 μL) for 3 min. Proteins were resolved on SDS-PAGE (12.5%) gels at 120 V for 2 h. The wet gel slabs were assayed by in-gel rhodamine fluorescence detection ($\lambda_{\text{ex}} = 523$ nm; $\lambda_{\text{em}} = 580$ nm, the red channel) and BODIPY-FL ($\lambda_{\text{ex}} = 488$ nm; $\lambda_{\text{em}} = 514$ nm, the green channel) by using a Thyphon scanner (GE Healthcare). For competition studies with Ada-Ahx₃-L₃-VS and bortezomib, EL4 protein lysate (20 μg) was first incubated with increasing competitor concentrations for 1 h at 37 °C, followed by labelling of the residual proteasome activity by Rh-SylA (1 μM end concentration). Coomassie blue staining of the gels afforded the loading control images.

Profiling of leukaemia cell lines was performed with total cell lysates of HL60, ARH77 and AMO-1 cells cultured in foetal calf serum supplemented RPMI-1640 with penicillin/streptomycin (1%). The medium for adapted cell lines in addition contained bortezomib (20 nM). Cell lysate protein (40 μg per lane) was loaded after incubation of Rh-SylA at a concentration of 5 μM for 1 h at 37 °C. Detection of labelling was performed with a fluorescence scanner FLA5000 (Fuji) at $\lambda_{\text{ex}} = 532$ nm and $\lambda_{\text{em}} = 580$ nm. Coomassie blue staining of the gels afforded the loading control images (see the Supporting Information).

Acknowledgements

Financial support from the Swiss National Science Foundation (grant 3100A0-115970, to R.D.), the Netherlands Organisation for Scientific Research (NWO, to H.O.) and the Netherlands Genomics Initiative (NGI, to B.F. and H.O.) is gratefully acknowledged.

Keywords: antitumor agents • leukemia • natural products • proteasome inhibitors • syrbactin

- [1] A. Herschko, A. Ciechanover, *Annu. Rev. Biochem.* **1998**, *67*, 425–479.
- [2] a) M. Groll, L. Ditzel, J. Löwe, D. Stock, M. Bochtler, H. D. Bartunik, R. Huber, *Nature* **1997**, *386*, 463–471; b) A. K. Nussbaum, T. P. Dick, W. Keilholz, M. Schirle, S. Stevanovic, K. Dietz, W. Heinemeyer, M. Groll, D. H. Wolf, R. Huber, H. G. Rammensee, H. Schild, *Proc. Natl. Acad. Sci. USA* **1998**, *95*, 12504–12509.
- [3] P.-M. Kloetzel, F. Ossendorp, *Curr. Opin. Immunol.* **2004**, *16*, 76–81.
- [4] B. S. Moore, A. S. Eustaquio, R. P. McGlinchey, *Curr. Opin. Chem. Biol.* **2008**, *12*, 434–440.
- [5] J. Sterz, I. von Metzler, J.-C. Hahne, B. Lamottke, J. Rademacher, U. Heider, E. Terpos, O. Sezer, *Expert Opin. Invest. Drugs* **2008**, *17*, 879–895.
- [6] C. Naujokat, D. Fuchs, C. Berges, *Biochim. Biophys. Acta* **2007**, *1773*, 1389–1397.
- [7] a) R. H. Feling, G. O. Buchanan, T. J. Mincer, C. A. Kauffman, P. R. Jensen, W. Fenical, *Angew. Chem.* **2003**, *115*, 369–371; *Angew. Chem. Int. Ed.* **2003**, *42*, 355–357; b) G. Fenteany, R. F. Staendert, W. S. Lane, S. Choi, E. J. Corey, S. L. Schreiber, *Science* **1995**, *268*, 726–731; c) L. Meng, R. Mohan, B. H. Kwok, M. Elofsson, N. Sin, C. M. Crews, *Proc. Natl. Acad. Sci. USA* **1999**, *96*, 10403–10408; d) J. Hines, M. Groll, M. Fahnestock, C. M. Crews, *Chem. Biol.* **2008**, *15*, 501–512; e) A. Asai, T. Tsujita, S. V. Sharma, Y. Yamashita, S. Akinaga, M. Funakoshi, H. Kobayashi, T. Mizukami, *Biochem. Pharmacol.* **2004**, *67*, 227–234; f) J. Kohno, Y. Koguchi, M. Nishio, K. Nakao, M. Kuroda, R. Shimizu, T. Ohnuki, S. Komatsubara, *J. Org. Chem.* **2000**, *65*, 990–995; g) I. Nickleit, S. Zender, F. Sasse, R. Geffers, G. Brandes, I. Sörensen, H. Steinmetz, S. Kubicka, T. Carlomagno, D. Menche, I. Gütemann, J. Buer, A. Gossler, M. P. Manns, M. Kalesse, R. Frank, N. P. Malek, *Cancer Cell* **2008**, *14*, 23–35.
- [8] M. Groll, B. Schellenberg, A. S. Bachmann, C. R. Archer, R. Huber, T. K. Powell, S. Lindow, M. Kaiser, R. Dudler, *Nature* **2008**, *452*, 755–758.
- [9] J. Clerc, M. Groll, D. J. Illich, A. S. Bachmann, R. Huber, B. Schellenberg, R. Dudler, M. Kaiser, *Proc. Natl. Acad. Sci. USA* **2009**, *106*, 6507–6512.

- [10] C. S. Coleman, J. P. Rocetes, D. J. Park, C. J. Wallick, B. J. Warn-Cramer, K. Michel, R. Dudler, A. S. Bachmann, *Cell. Prolif.* **2006**, *39*, 599–609.
- [11] a) B. F. Cravatt, A. T. Wright, J. W. Kozarich, *Annu. Rev. Biochem.* **2008**, *77*, 383–414; b) M. Fonovic, M. Bogoy, *Expert Rev. Proteomics* **2008**, *5*, 721–730; c) T. Böttcher, S. A. Sieber, *Angew. Chem.* **2008**, *120*, 4677–4680; *Angew. Chem. Int. Ed.* **2008**, *47*, 4600–4603.
- [12] a) M. Bogoy, *Methods Enzymol.* **2005**, *399*, 609–622; b) M. Bogoy, S. Shin, J. S. McMaster, H. L. Ploegh, *Chem. Biol.* **1998**, *5*, 307–320; c) T. Nazif, M. Bogoy, *Proc. Natl. Acad. Sci. USA* **2001**, *98*, 2967–2972; d) M. Verdoes, B. I. Florea, V. Menendez-Benito, C. J. Maynard, M. D. Witte, W. A. van der Linden, A. M. C. H. van den Nieuwendijk, T. Hofmann, C. R. Berkens, F. W. B. van Leeuwen, T. A. Groothuis, M. A. Leeuwenburg, H. Ovaa, J. J. Neefjes, D. V. Filippov, G. A. van der Marel, N. P. Dantuma, H. S. Overkleeft, *Chem. Biol.* **2006**, *13*, 1217–1226; e) M. Verdoes, U. Hill-aert, B. I. Florea, M. Sae-Heng, M. D. Risseuw, D. V. Filippov, G. A. van der Marel, H. S. Overkleeft, *Bioorg. Med. Chem. Lett.* **2007**, *17*, 6169–6171.
- [13] a) C. R. Berkens, M. Verdoes, E. Lichtman, E. Fiebigler, B. M. Kessler, K. C. Anderson, H. L. Ploegh, H. Ovaa, P. J. Galardy, *Nat. Methods* **2005**, *2*, 357–362; b) M. Groll, C. R. Berkens, H. L. Ploegh, H. Ovaa, *Structure* **2006**, *14*, 451–456.
- [14] T. Rückrich, M. Kraus, J. Gogel, A. Beck, H. Ovaa, M. Verdoes, H. S. Overkleeft, H. Kalbacher, C. Driessen, *Leukemia* **2009**, *23*, 1098–1105.
- [15] a) R. Oerlemans, N. E. Franke, Y. G. Assaraf, J. Cloos, I. van Zantwijk, C. R. Berkens, G. L. Scheffer, K. Debipersad, K. Vojtekova, C. Lemos, J. W. van der Heijden, B. Ylstra, G. J. Peters, G. L. Kaspers, B. A. Dijkmans, R. J. Scheper, G. Jansen, *Blood* **2008**, *112*, 2489–2499; b) S. Lü, J. Yang, X. Song, S. Gong, H. Zhou, L. Guo, N. Song, X. Bao, P. Chen, J. Wang, *J. Pharmacol. Exp. Ther.* **2008**, *326*, 423–431.
- [16] S. Meiners, A. Ludwig, V. Stangl, K. Stangl, *Med. Res. Rev.* **2008**, *28*, 309–327.
- [17] a) M. Kaiser, M. Groll, C. Renner, R. Huber, L. Moroder, *Angew. Chem.* **2002**, *114*, 817–820; *Angew. Chem. Int. Ed.* **2002**, *41*, 780–783; b) M. Kaiser, M. Groll, C. Siciliano, I. Assfalg-Machleidt, E. Weyher, J. Kohno, A. G. Milbradt, C. Renner, R. Huber, L. Moroder, *ChemBioChem* **2004**, *5*, 1256–1266; c) M. Kaiser, A. G. Milbradt, C. Siciliano, I. Assfalg-Machleidt, W. Machleidt, M. Groll, C. Renner, L. Moroder, *Chem. Biodiversity* **2004**, *1*, 161–173.

Received: July 3, 2009

Published online on September 11, 2009